toxics

MDPI

Article

Evaluation of Apical and Molecular Effects of Algae *Pseudokirchneriella subcapitata* to Cerium Oxide Nanoparticles

Ntombikayise Mahaye and Ndeke Musee *

Emerging Contaminants Ecological and Risk Assessment (ECERA) Research Group, Department of Chemical Engineering, University of Pretoria, Pretoria 0028, South Africa; mahaye.ntombi@gmail.com
* Correspondence: ndeke.musee@up.ac.za or museen2012@gmail.com

Abstract: Cerium oxide engineered nanoparticles ($nCeO_2$) are widely used in various applications and are, also, increasingly being detected in different environmental matrixes. However, their impacts on the aquatic environment remain poorly quantified. Hence, there is a need to investigate their effects on non-target aquatic organisms. Here, we evaluated the cytotoxic and genotoxic effects of <25 nm uncoated-$nCeO_2$ on algae *Pseudokirchneriella subcapitata*. Apical (growth and chlorophyll *a* (Chl *a*) content) and genotoxic effects were investigated at 62.5–1000 µg/L after 72 and 168 h. Results demonstrated that $nCeO_2$ induced significant growth inhibition after 72 h and promotion post 96–168 h. Conversely, $nCeO_2$ induced enhanced Chl *a* content post 72 h, but no significant changes were observed between $nCeO_2$–exposed and control samples after 168 h. Hence, the results indicate *P. subcapitata* photosynthetic system recovery ability to $nCeO_2$ effects under chronic-exposure conditions. RAPD-PCR profiles showed the appearance and/or disappearance of normal bands relative to controls; indicative of DNA damage and/or DNA mutation. Unlike cell recovery observed post 96 h, DNA damage persisted over 168 h. Thus, sub-lethal $nCeO_2$-induced toxicological effects may pose a more serious threat to algae than at present anticipated.

Keywords: *Pseudokirchneriella subcapitata*; cerium oxide nanoparticles; DNA stability; RAPD-PCR; growth effect; chlorophyll *a* content

Citation: Mahaye, N.; Musee, N. Evaluation of Apical and Molecular Effects of Algae *Pseudokirchneriella subcapitata* to Cerium Oxide Nanoparticles. *Toxics* **2023**, *11*, 283. https://doi.org/10.3390/toxics11030283

Academic Editor: Farhan R. Khan

Received: 30 January 2023
Revised: 9 March 2023
Accepted: 13 March 2023
Published: 19 March 2023

1. Introduction

Cerium oxide engineered nanoparticles ($nCeO_2$) are a class of emerging contaminants with unique properties when compared to their bulk counterpart. These properties include redox activity, scavenging of free radicals, and inhibition of biofilm formation [1]. As a result, $nCeO_2$ find widespread applications, e.g., in sunscreens as UV absorbent [2], fuel additives [3], catalysis [4,5], biomedicine [6], and nano-pharmacy [7]. Estimates indicate that $nCeO_2$ global production to be 100 and 1000 tons/year [8] and may have increased to 7500–10,000 tons/year [9,10]. Since $nCeO_2$ is widely used as an additive for diesel fuels, for instance, it is, therefore, among likely engineered nanoparticles (ENPs) of ecological concern in the natural environment [11]. In addition, $nCeO_2$ has been quantified in various environmental matrixes using modelling (e.g., 0.1 µg/L in surface waters [12] and experimental (0.4–5.2 ng/L in surface waters [13]) approaches. However, the environmental implications of $nCeO_2$ remain poorly understood. Yet, it is among the top ten priority ENPs identified both for the evaluation of human health and environmental safety effects [14].

Following the release of $nCeO_2$ into the ecosystems, they may accumulate in the aquatic systems linked to their transformation processes including aggregation, sedimentation, and low degradation rate. This, in turn, increases their uptake, accumulation, and bio-magnification in the food chain [15] and inevitable interactions with different classes of aquatic organisms [16]. Therefore, understanding the impact of $nCeO_2$ on aquatic biota especially organisms that represent the base of the trophic chain is of ecological significance.

Algae are unicellular organisms and primary producers that play a vital role in the structure and functioning of ecosystems and are susceptible test species to environmental

pollutants [17]. In fact, to date, several studies have documented the deleterious effects of $nCeO_2$ on algae [16,18–21]. For example, following exposure of freshwater algae *Pseudokirchneriella subcapitata* over 72 h to poly acrylic acid (PAA) coated-$nCeO_2$ (4–10 nm; spherical shaped) exposure at concentrations of 15–200 µg/L, significant oxidative stress response was observed, and EC_{50} of 24 µg/L was reported owing to the ENPs' dispersion and bioavailability [18]. Most effect studies of $nCeO_2$ on algae were conducted using apical endpoints (e.g., growth effects), with only a handful at the sub-lethal level [22,23] and at low environmentally relevant concentrations (ng/L to µg/L).

Remarkably, at sub-lethal exposure concentrations, the ENPs effects at the morphological level generally are masked but are apparent at the molecular level [24–27]. For instance, Taylor et al. [26] assessed the molecular and phenotypic toxic effects of 4–5 nm polyvinylpyrrolidone (PVP)-coated $nCeO_2$ (0.5–80,000 µg/L) on freshwater algae *Chlamydomonas reinhardtii* using transcriptomic and metabolomic techniques. Results demonstrated the internalization of mono-dispersed PVP-$nCeO_2$ by intracellular vesicles, but no growth inhibition was observed irrespective of exposure concentration. Additionally, molecular perturbations (e.g., down-regulation of photosynthesis) were observed only at very high concentrations (>10,000 µg/L). Based on their results, the authors recommended the assessment of longer-term exposure and consequences of internalization within the aquatic food chain, bioavailability, and potential toxicity of $nCeO_2$ to primary consumers [26]. Importantly, ENPs may undergo dissolution upon exposure to aqueous media. These metal ions in suspensions of metal-based ENPs play an important role in determining toxicity of ENPs [28]. For example, following exposure of algae to $nCeO_2$, the Ce concentration in the medium decreased [20]. These results showed that $nCeO_2$ and Ce ions might adsorb on the algal cell surface or enter algal cells. The intracellular available Ce content in the 50 mg/L treatment was significantly higher than the control, which might do harm to algal cells. The authors of [29] reported that Ce^{3+} of 0.5~10 mg/L could inhibit the growth of *Anabaena flosaquae*. Meanwhile, Ce could enter the cell of *Arabidopsis thaliana* and destroy the ultrastructure of cells [30].

Conversely, Angel et al. [31] reported IC_{50} of *P. subcapitata* of dissolved Ce (0.63 mg/L) to be much higher than the measured solubility. Thus, they considered that the dissolved Ce could hardly cause the observed toxicity. In a study by Wu et al. [20], the intracellular Ce content of 50 mg/L $nCeO_2$ treatment was the highest among all the treatments, which might be responsible for the growth inhibition and toxicity effects of $nCeO_2$. The authors concluded that, however, it is difficult to determine whether the adsorption of $nCeO_2$ or the intracellular Ce contribute more to the toxicity of $nCeO_2$ [20].

Overall, documented studies have demonstrated the importance of molecular studies towards robust risk assessment of ENPs on the aquatic biota. This is why, in recent years, ecotoxicological studies have shifted from apical to molecular endpoints including for ENPs [22]. This is because changes at the molecular level have been demonstrated to induce deleterious long-term ecological implications [32] not observable at an organismal level. Among the molecular effect assays, includes genotoxicity-based methods. For example, random amplified polymorphic deoxyribonucleic acid by Polymerase Chain Reaction (RAPD-PCR) analysis has been widely applied to assess the genotoxicity of ENPs to aquatic biota, e.g., algae [27], aquatic invertebrates [33], and fish [34,35]. The key advantage of RAPD-PCR analysis is its ability to screen changes in DNA profiles and evaluate genomic stability. For instance, Mahaye and colleagues recently applied RAPD-PCR and the apurinic/apyrimidinic (AP) sites techniques to evaluate the genotoxic effects of differently coated gold nanoparticles (nAu) on algae *P. subcapitata* over 168 h. The genotoxicity results demonstrated significant toxicity of nAu on algae including on samples where undesirable effects were undetectable from the apical endpoints (e.g., growth effect and chlorophyll *a* (Chl *a*) content) [27].

At present, there are a lack of genotoxicity data pertaining to the interactions between $nCeO_2$ and algae unlike in the case of crustaceans and fish, especially for $nTiO_2$ and nAg as the most studied organisms and ENPs, respectively [22]. To address this knowledge gap,

herein we investigated the impact of $nCeO_2$ on freshwater microalgae *P. subcapitata* at low exposure concentrations in the μg/L range as their use increases; thus, they are likely to be found in the actual environment. The study specific objectives were to assess the effects of $nCeO_2$ (at concentrations of 62.5–1000 μg/L) on *P. subcapitata*: (i) at apical endpoints including growth effect and Chl *a* content and (ii) on DNA integrity using RAPD-PCR analysis in 10% Blue Green algae-11 (BG-11) medium after 72 and 168 h. The toxicological effects observed from the molecular and apical endpoints assessments were compared or linked to gain better understanding on the effects of $nCeO_2$ on algae under chronic exposure conditions.

2. Materials and Methods

2.1. Characterization of $nCeO_2$

Uncoated $nCeO_2$ in dispersion (<25 nm particle size, 10 wt.% in H_2O) were purchased from Sigma Aldrich (Johannesburg, South Africa). Size and morphology were characterized as previously described by Mahaye [36]. Hydrodynamic diameter (HDD) and zeta (ζ) potential of $nCeO_2$ in de-ionized water (DI water) (15 MΩ/cm) and 10% Blue Green algae-11 media (herein referred to as BG-11 media) [37] were measured using dynamic light scattering (DLS) (Malvern Zetasizer Nano ZS, Malvern, UK). Measurements for the ζ-potential and HDD were taken at 0, 2, 6, 24, 48, and 72 h in triplicate. The HDD and ζ-potential measurements in DI water and BG-11 media were only done at 1000 μg/L $nCeO_2$. This is because $nCeO_2$ at concentrations <1000 μg/L were below the detection limit using the Zetasizer.

2.2. Preparation of Exposure Media and Concentrations

Algal experiments were conducted in BG-11 media (media preparation and composition details are listed in Section SI-1 and Table S1, respectively, in the supporting information) following Direct Estimation of Ecological Effects Potential (DEEEP) toxicity testing protocols [37]. The media was stored at 4 °C under dark conditions before use. The $nCeO_2$ exposure concentrations of 62.5, 125, 250, 500, and 1000 μg/L were prepared in BG-11 media in triplicate and ultra-sonicated for 30 min before carrying out the exposure experiments.

2.3. Test Organisms

The Algaltoxkit F^{TM} kit (MicroBioTests Inc., Gent, Belgium) was purchased from Tox-Solutions (Johannesburg, South Africa). Algaltoxkit F contains all the materials needed to perform a 72 h growth inhibition tests with the freshwater microalgae *P. subcapitata* (former names: *Selenastrum capricornutum* and *Raphidocelis subcapitata*). This algal toxicity test was carried strictly in adherence to ISO Standard 8692 and OECD Guideline 201 protocols. The de-immobilization of *P. subcapitata* from the beads was performed in accordance with the manufacturer's instructions. In this study, stock cultures were incubated under controlled conditions (temperature: 25 ± 1 °C; light intensity: 6000 Lux; 12:12 h light: dark cycle and shaken continuously at 100 rpm) for 5–7 d to obtain exponentially growing *P. subcapitata*.

2.4. Cytotoxic Effects of $nCeO_2$ on P. subcapitata

Preparation of the algal test was performed as outlined in Mahaye et al. [27]. Reference tests aimed to ascertain the sensitivity of algae growth are described in Section SI-2. Inoculum was prepared by harvesting exponentially growing *P. subcapitata* cells. Cells from a 5–7 d old stock culture prepared in Section 2.3 were transferred as 1 mL volume into Eppendorf tubes and centrifuged at 10,000 rpm for 10 min. The supernatant was decanted, and the algal cells were re-suspended in 0.1 mL phosphate-buffered saline (PBS). The centrifugation and decanting steps were repeated twice. The volume of stock culture

required and the cell density of algal inoculum required per experiment in test and control wells were calculated using the following expression:

$$Volume\ (\mathrm{mL}) = \frac{no.\ of\ flasks\ used \times \frac{vol}{flask} \times 200000\ cells/mL}{Cell\ density\ (\mathrm{cells/mL})\ in\ the\ stock\ culture} \quad (1)$$

where vol/flask is the volume of test solution per flask and cells/mL is the cell density in the inoculum given by the following expression [38]:

$$\mathrm{Cells/mL} = e^{\frac{ln\lambda_{684}+16.439}{1.0219}} \quad (2)$$

where λ_{684} is the optical density (OD) at 684 nm.

In the final step, algal cells were re-suspended and mixed well in 10% BG-11 media and the cell density in the inoculum was measured before the experiment was initiated. For each test, 200,000 cells/mL sample was required. Tests were carried out in 2 mL volumes in 24-well microplates with 1.8 mL test sample (or de-ionised water for the control), with 0.2 mL of the inoculum and algal medium. Thereafter, it was incubated at the same conditions as the stock culture for 168 h. *P. subcapitata* exposures to $nCeO_2$ were conducted following the standard algal test of 72 [37], or 96 h [39] with slight modifications. First, the exposure time was increased from 96 to 168 h to gain insights on likely effects under chronic conditions. The standard US EPA flask test method [39] yielded inadequate biomass for genotoxicity analysis as it requires only 10,000 cells/mL as initial inoculum. Thus, to generate sufficient biomass for genotoxicity analysis, we used the DEEEP toxicity testing protocol [37]. This protocol requires an inoculum of 200,000 cells/mL, which, in turn, generated adequate biomass for DNA damage analysis [27].

For negative controls, exposures for algae were done without $nCeO_2$. All experiments were done in triplicate. Exponentially growing *P. subcapitata* were exposed to five concentrations of $nCeO_2$ (62.5, 125, 250, 500 and 1000 µg/L) for 168 h, in a 24-well microplate system, under defined conditions outlined in Section 2.3. Exposure concentrations were selected based on the detected or predicted environmental concentrations from the previous studies. For example, $nCeO_2$ concentrations of 0.3–230 µg/L [40] and 0.04–0.27 µg/L [41] were reported in freshwater. The ENPs' concentrations in freshwater are predicted to reach six-fold higher by the year 2050 [42]. Thus, in this study, the selected exposure concentrations cover both current and plausible future predicted concentrations of $nCeO_2$ in freshwater systems.

After the experiments were initiated, the cell density (in the form of optical density) was measured at 684 nm every 24 h for 168 h using a microplate reader (FLUOstar Omega BMG Labtech, Ortenberg, Germany). Briefly, the wavelength of 684 nm used here was adopted from Rodrigues et al. [38] and has been successfully used on ENPs-exposed *P. subcapitata* studies [27,43,44]. After 72 and 168 h exposure periods, Chl *a* content was determined following a protocol by Harris [45]. Briefly, 1 mL of the control and exposed algal cells were centrifuged for 10 min at 13,000 rpm, and the pellet was washed using DI water. The algal cells pellet was suspended in 95% ethanol, vortexed for 2 min, kept at 4 °C for 30 min and centrifuged at 13,000 rpm for 2 min. The supernatant was analysed for Chl *a* content using a UV-Vis spectrophotometer (HACH, Loveland, CO, USA) at wavelengths of 665 and 649 nm. The content of Chl *a* was then calculated using the expression:

$$\mathrm{Chl}\ a = 13.70A_{665} - 5.76A_{649} \quad (3)$$

where A_{665} and A_{649} are the OD values (n =3) at wavelengths of 665 nm and 649 nm, respectively.

2.5. DNA Damage and Estimation of Genomic Template Stability

DNA isolation, visualization, and amplification were done as described in Mahaye et al. [27], and details are set out in Section SI-3. Briefly, exponentially growing *P. subcapitata* were exposed to three $nCeO_2$ concentrations at 62.5, 250, and 1000 µg/L as described in Section 2.3. RAPD-PCR data analysis was performed by comparing the PCR product profiles for $nCeO_2$-treated sample with the control samples. The genomic template stability percentage (GTS%) was calculated using the following Equation [46]:

$$\mathrm{GTS} = \left(1 - \frac{a}{n}\right) \times 100 \quad (4)$$

where a is the average number of RAPD polymorphic bands detected in ENPs-treated samples and n is the total bands in the controls. Polymorphisms in RAPD profiles include deletion of a normal band and induction of a new band in comparison to the control RAPD profiles. GTS percentage of $nCeO_2$ -treated samples was calculated and changes of genomic stability were expressed as a percentage of controls set at 100%.

2.6. Data Analysis

All measurements were performed in triplicate, and the results were expressed as mean ± standard deviation (SD). Statistical analysis was performed using GraphPad Prism Software version 9.3.0 (GraphPad Software, San Diego, CA, USA). One-way analysis of variance (ANOVA) followed by Dunnett's post hoc test was used to evaluate statistical differences between $nCeO_2$-exposed samples and the controls. Differences between samples were considered statistically significant when $p \leq 0.05$.

3. Results and Discussion

3.1. Characterization of $nCeO_2$

$nCeO_2$ had non-uniform triangular, tetrahedral, and hexagonal shapes (Figure S1a), with diameters of 15–50 nm due to the asymmetry of the morphology. Although most $nCeO_2$ were <25 nm, larger and compact crystalline structures were also observed (Figure S1b). Figure S1c depicts the particle size distribution of $nCeO_2$ at 1000 µg/L in BG-11 media measured using DLS. The presence of agglomerates >25 nm showed that the primary particle sizes could not be attained even after ultrasonication, as previously documented in other works [47–50]. $nCeO_2$ aggregated immediately following introduction into both DI water and BG-11 media (Figure 1A). After 24–72 h exposure, aggregation was higher in BG-11 media compared to DI water (Figure 1A). The higher aggregation was likely due to high ionic strength of BG-11 media relative to DI water as previously documented [51,52].

In an earlier work, uncoated $nCeO_2$ sized 28 nm was observed to form aggregates of 200–300 nm in ultrapure water [49]. Here, the observed aggregation in BG-11 media show a good agreement with the behaviour of uncoated-$nCeO_2$ as documented in other algal ecotoxicity media, e.g., synthetic freshwater algal media [31,53], OECD TG 201 [54] and Dutch Standard (DS) medium [55]. For example, 20 nm uncoated-$nCeO_2$ immediately agglomerated to 218 nm in DS medium, which is ten-fold higher than the primary size [55]. Negative ζ-potential values for 1000 µg/L $nCeO_2$ were observed in both media types over 72 h and at a narrow range of −8 to −16 mV (Figure 1B). These low ζ-potential values indicate $nCeO_2$ instability and are consistent with the rapid agglomeration observed in both DI water and BG-11 media (Figure 1A). This is because ζ-potential values should be ±30 mV to stabilize ENPs suspensions [56,57].

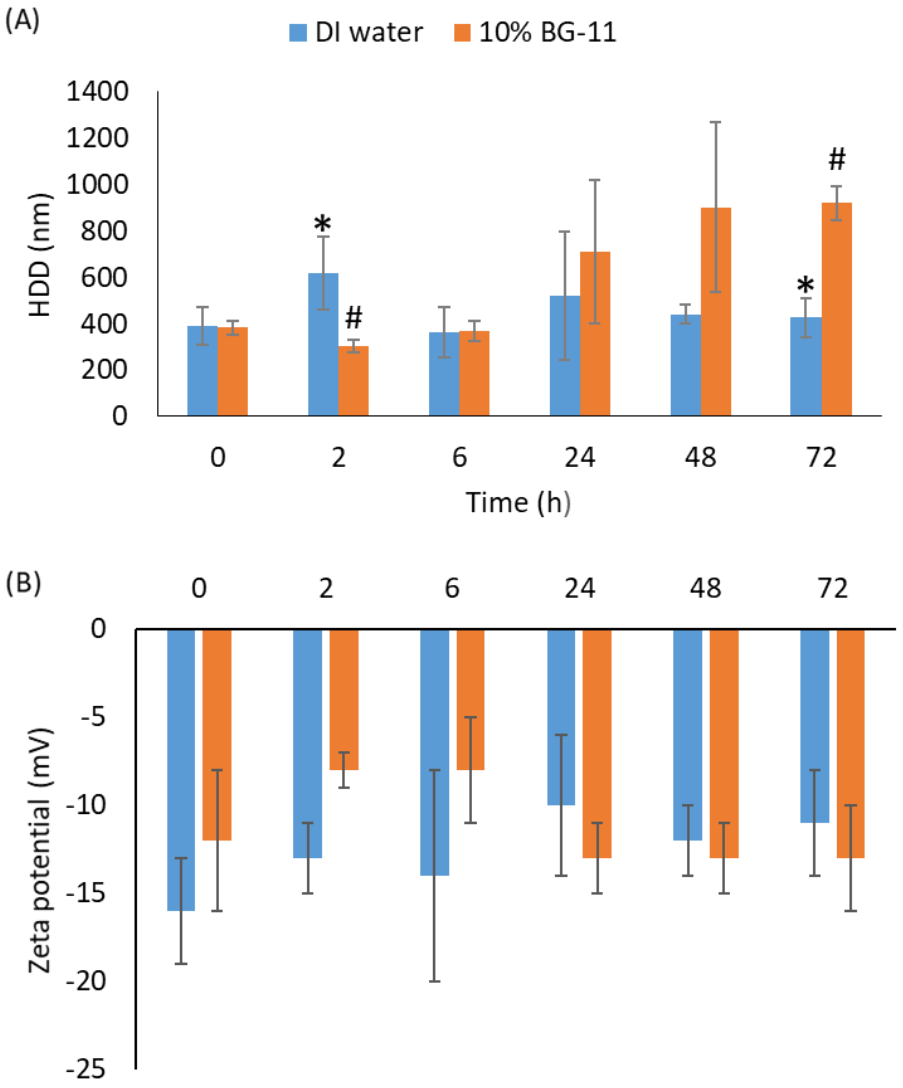

Figure 1. The (**A**) HDD and (**B**) ζ potential at 1000 µg/L of $nCeO_2$ in DI water and BG−11 media measured using DLS over 72 h. Data are presented as mean ± standard deviation (SD). Different symbols denote significant differences ($p < 0.05$) between DI water and BG-11 media per time period analysed using Two-way ANOVA with Tukey's multiple comparisons test.

3.2. *Effect of $nCeO_2$ on Algal Growth*

A positive control was performed using potassium dichromate ($K_2Cr_2O_7$) as a reference toxicant, and results are presented in Figure S2. Results in Figure 2 demonstrates the growth effect of $nCeO_2$ on algae over 168 h. Remarkably, $nCeO_2$ had no significant effect on algal growth following exposure after 24 and 48 h but induced significant growth inhibition after 96 h relative to the controls. Growth promotion was, however, observed after 96 h and significantly higher after 144 and 168 h, compared to the controls. Any modification of algae growth may, subsequently, affect higher trophic levels [58]. For instance, they may lead to altered species composition and habitat structure [59] and, as a result, compromise ecological integrity. Among ecological functioning, aspects that may be adversely affected include the extinction of sensitive algal species and macrophytes, or higher growth may outcompete other biological life forms with consequent undesirable perturbations on the food chain and nutrient recycling, among others.

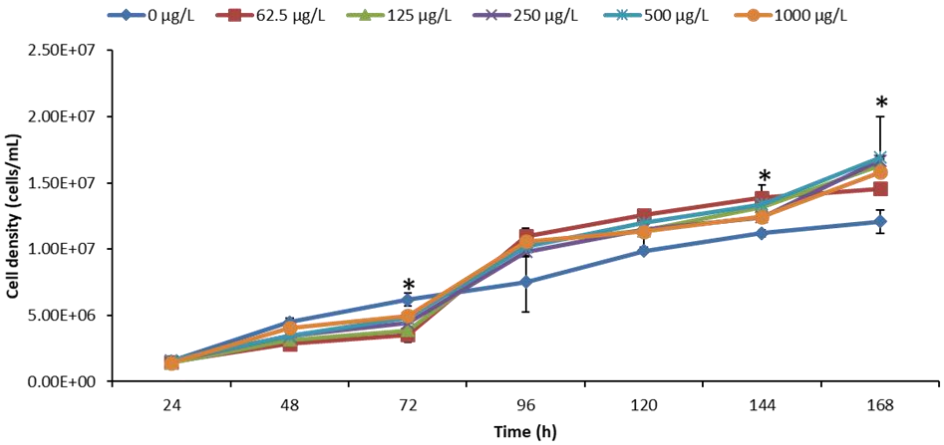

Figure 2. Cell density of *P. subcapitata* at different exposure concentrations of $nCeO_2$. Results were reported as mean ± standard deviation where $n = 3$. The asterisk denotes significant differences ($p < 0.05$) between $nCeO_2$-treated and control samples.

Similar to our findings, Dedman et al. [60] investigated growth effects of *Prochlorococcus* sp. MED4 by <25 nm $nCeO_2$ over 72 h (1–100 µg/L) and extended exposure time of 240 h at environmentally relevant (1–100 µg/L) and supra-environmental (1–100 mg/L) concentrations. Results indicated significant reduction of *Prochlorococcus* cell density (up to 68.8%) at 100 µg/L $nCeO_2$ after 72 h. The lowest tested concentrations of 1 and 10 µg/L induced no observable effect on *Prochlorococcus* growth irrespective of exposure time (72 and 240 h). However, 1 µg/L induced about 38.8% increase in cell density relative to the control in nutrient-enriched media after 240 h. Exposure to supra-environmental $nCeO_2$ concentrations (i.e., 100 mg/L) yielded a significant decline in cell density of up to 95.7 and 82.7%, respectively, in natural oligotrophic seawater and nutrient-enriched media. The observed cell decline was attributed to the extensive aggregation behaviour of $nCeO_2$ upon entry into natural seawater and hetero-aggregation with algae [60]. In addition, direct contact of $nCeO_2$ with algae was reported previously to be responsible for toxicity and to cause membrane damage of *P. subcapitata* [53]. Further, an increase in intracellular reactive oxygen species (ROS) was observed in algae [19]. Intracellular ROS plays a role in the inhibition of photosynthesis and can indicate oxidative damage [61].

Previous studies have demonstrated the absence of uptake of uncoated and agglomerated $nCeO_2$ in algae [31,61]. The lack of ENPs uptake was linked to the formation of agglomerates that exceeded the pore sizes (ranges between 5 and 20 nm) of the algal cell wall [62], which, in turn, impeded plausible uptake by algae. Here, the observed agglomerates (up to 918 ± 74 nm) exceeded the algal cell wall pore sizes and, therefore, uptake was reasonably unlikely. Thus, growth inhibition observed was possibly due to the entrapment of algal cells by ENPs agglomerates. As a result, this may have reduced the light and nutrients' availability to the entrapped algal cells with concomitant growth inhibition. Previously, algal growth inhibition was observed to result from physical removal due to co-aggregation and co-sedimentation with $nCeO_2$, as opposed to the toxicological and cell death effect [60].

$nCeO_2$ effects on algae have been observed to be concentration- and exposure duration-dependent [60,63,64]. For example, growth inhibition of the algae *Microcystis aeruginosa* following exposure to <25 nm $nCeO_2$ (1, 10 and 50 mg/L) in BG-11 media over 72 h was observed to be exposure-duration dependent [64]. No significant differences were observed between the controls and $nCeO_2$-treated samples after 24 h. However, after 48 h at concentrations of 1 and 10 mg/L $nCeO_2$, results indicated algal growth promotion, but 50 mg/L induced significant growth inhibition of *M. aeruginosa* [64]. After 72 h, no algal growth was observed at 1 mg/L, increased significantly at 10 mg/L, but a significant inhibition was apparent at 50 mg/L $nCeO_2$ [64]. Deng and colleagues reported similar results, where they observed induction of growth promotion on marine diatom *Phaeodactylum tricornutum*

at low $nCeO_2$ concentrations of ≤5 mg/L, whereas growth inhibition at ≥10 mg/L was documented [63].

Herein, the observed recovery of algal population under extended exposure conditions may be attributed to a decrease in $nCeO_2$ concentrations bioavailable for algae (Figure S3) as ENPs formed aggregates (Figure 1A and Figure S1) and underwent sedimentation in BG-11 media over time. Furthermore, recovery of the populations was attributed to the algae defence mechanisms in response to ENPs exposure. For example, algae employ a variety of defence mechanisms including activation of the antioxidative defence system to eliminate reactive oxygen species (ROS) [65,66], excretion of biomolecules to form a protective layer [67], and intracellular processes to decrease the cellular content of ENPs [68]. Thus, the findings herein and others demonstrates that the likely environmental risk of $nCeO_2$ on algae appear to be low at the morphological level even under extended exposure conditions.

3.3. Effect of $nCeO_2$ on Chl *a* Content

Photosynthesis is a key process in algae and quantified as Chl *a* content–an efficient indicator for physiological health status of algal cells [69,70]. Figure 3 demonstrates Chl *a* content of *P. subcapitata* for $nCeO_2$- and non-exposed samples after 72 and 168 h. Contrary to the algal growth inhibition observed up to 72 h (Figure 2), findings in Figure 3 demonstrate that $nCeO_2$ enhanced Chl *a* content ($p < 0.05$) compared to the controls over the same period, but remarkably independent of the exposure concentration. In an earlier work, increase in Chl *a* content relative to controls were observed on *C. reinhardtii* following exposure to 4 nm-sized uncoated-$nCeO_2$ at 0.1–50 mg/L [16]. The observed increase in Chl *a* was associated with an interruption of the electron transport at the acceptor side of photosystem PSII [71,72]. Furthermore, other metal oxide ENPs, e.g., nZnO and $nTiO_2$, were observed to enhance algal growth and Chl *a* content in *Picochlorum* sp. [73] and *P. subcapitata* [74–76]. The basis for Chl *a* content promotion was plausibly due to the conversion of other forms of pigments (e.g., Chl *b* content) into Chl *a* content as a response to ROS following exposure to ENPs [77]. Gui et al. [78] reported significant increases in Chl content after plant exposure to 10, 50, and 100 mg/kg $nCeO_2$ after 40 d. On day 50, only 50 and 100 mg/kg $nCeO_2$ concentrations increased the Chl content. Similar to our findings after 168 h, at the harvest stage, all of $nCeO_2$ treatments had no more significant difference [78]. After $nCeO_2$ (200 mg/L) exposure for 1 w, the Chl *a* and Chl *b* contents of rice seedlings did not show any significant changes relative to the control [79].

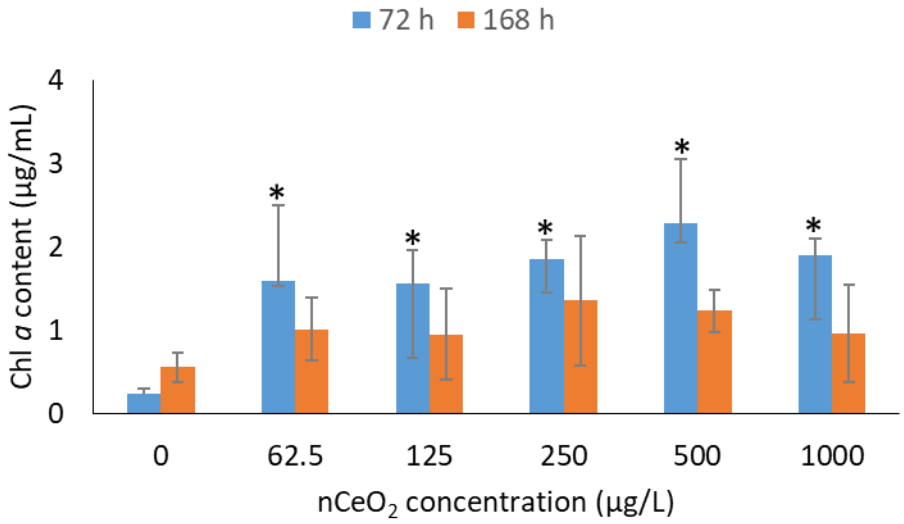

Figure 3. Chl *a* content of *P. subcapitata* at different $nCeO_2$ exposure concentrations. Results are reported as mean ± standard deviation where $n = 3$ and asterisk denotes significant differences ($p \leq 0.05$) between exposed and non-exposed samples after 72 h.

After 168 h, no significant changes in Chl *a* content were observed between $nCeO_2$–exposed and control samples. These findings indicated that the photosynthetic system of *P. subcapitata* can tolerate the presence of $nCeO_2$ under chronic exposure conditions. In contrast to growth promotion post 96 to 168 h, a reduction in Chl *a* content was observed after 168 h compared to 72 h. Similarly, the findings of Zhao et al. [64] showed that 10 mg/L $nCeO_2$ promoted algal growth, but it was also accompanied by a slight inhibition of photosynthetic yield. In addition, exposure of *P. subcapitata* to <50 nm uncoated-$nCeO_2$ at 0.01–100 mg/L for 72 h showed a dual response, firstly, with 20–50% stimulation in Chl *a* content at lower concentration range of 0.01–1 mg/L and, secondly, a significant inhibition was observed at higher concentrations of 10–100 mg/L [19]. The primary cause of the observed photosynthetic inhibition was due to excessive levels of ROS formation, which, in turn, induced oxidative damage as evidenced by lipid peroxidation data [19,69]. Furthermore, ENPs bound onto algal membranes were observed to induce a shading effect or membrane damage and, in turn, inhibit the photosynthesis process [80–82]. To date, physical restraints and oxidative stress were reported to be mechanisms responsible for ENPs toxicity to algae [83]. The entrapment of algal cells by large ENP aggregates not only reduces light available for photosynthesis, but also prevents uptake of nutrients [70]. Among available ENP-toxicity mechanisms, a large number of studies indicated oxidative stress as the dominant toxicity mechanism of ENPs to algae [84]. For instance, Chen et al. [85] conducted a meta-analysis study, and the results showed that the level of ROS significantly increased by 90% in the presence of ENPs, indicating the accumulation of excess ROS in algal cells which ultimately caused oxidative stress. Additionally, ENP-induced ROS accumulation was not significantly influenced by ENP surface modification ($p = 0.103$) but was strongly influenced by the ENP type ($p = 0.044$), ENP dose ($p = 0.001$), and algae species ($p < 0.001$). Findings of the current study point to the need to consider long-term exposure conditions, as the results of $nCeO_2$ on algae appear to be exposure time dependent.

3.4. DNA Damage and Estimation of Genomic Template Stability

Cytotoxicity study (growth effect and Chl *a* content) results did not differ as a function of $nCeO_2$ exposure concentration compared to the control (Figures 2 and 3). Thus, genotoxicity studies using RAPD-PCR method were conducted at 62.5, 250, and 1000 µg/L $nCeO_2$ representing the lowest, median, and highest concentrations, correspondingly. The results in Figure 4 show the RAPD-PCR profiles of isolated genomic DNA from $nCeO_2$-treated and untreated samples. These profiles were also used to analyse GST% (Equation (2)). A negative control (no DNA) was included to ascertain whether any band observed was attributable to DNA amplification.

RAPD-PCR profiles for $nCeO_2$ treated algae using OPB1 primer were markedly different from those of the controls (Figure 4a). Modifications in DNA were in the form of appearance of two new clear bands at ±200–500 bp and disappearance of a normal clear band observed at ±900 bp in the controls (Figure 4a). Specifically, we observed various size ranges for $nCeO_2$ treated samples compared to the controls. Notably, the DNA strands in the form of clear bands for $nCeO_2$ treated samples were shorter (±200–500 bp) compared to the controls (±900 bp), indicating that the DNA of the control samples was more intact compared to one from $nCeO_2$ treated algae. The observed DNA modifications were neither concentration nor time dependent, indicating that $nCeO_2$-induced 72 h-DNA damage persisted over 168 h. The observed modifications of RAPD-PCR profiles were likely due to one or a combination of variant events, e.g., DNA adducts, DNA breakage and mutation (e.g., point mutations and large rearrangements) [46,86]. The OPB14 primer produced similar RAPD profiles for controls and $nCeO_2$-treated algal DNA irrespective of exposure concentration and time (Figure 4b), with a GTS of 100%. Similarly, RAPD profile analysis after exposure of *Pseudomonas putida* to aluminium oxide ENPs (nAl_2O_3) showed no difference to the control, pointing to the induction of the DNA repair mechanisms [87]. Furthermore, the findings demonstrated primer-dependent genotoxicity. Previously, expo-

sure of *P. putida* bacteria to <50 nm nAl_2O_3 using four primers, e.g., OPA2, OPA10, OPA9, and OPA18 also showed primer-dependent DNA damage [87]. Results obtained using primer OPA2, demonstrated the most significant mutagenic action of nAl_2O_3, whereas the OPA10 and OPA18 primers RAPD band profiles showed the least mutagenic effect with small variations between ENPs-treated samples and control.

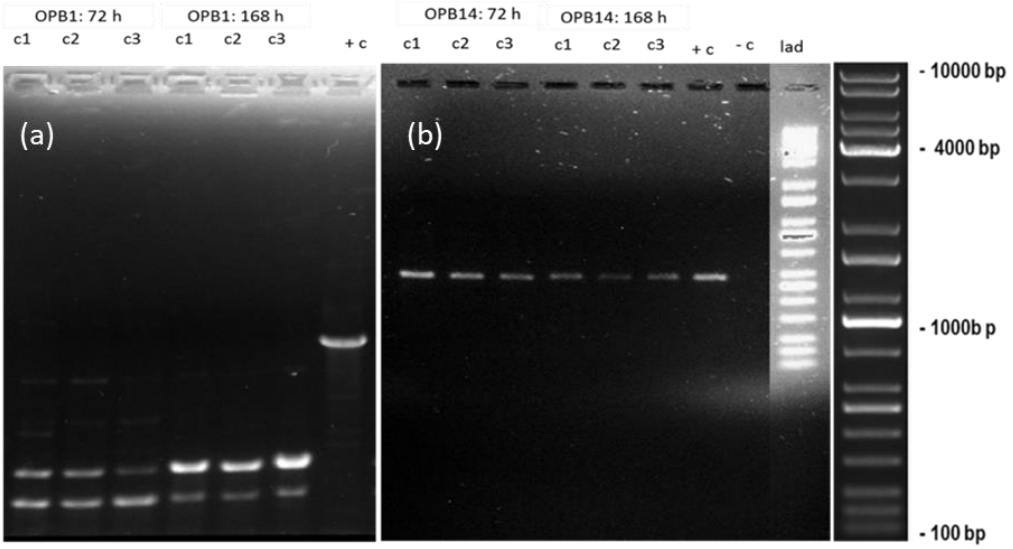

Figure 4. RAPD-PCR profiles generated using (**a**) OPB1 primer and (**b**) OPB14 primer after 72 and 168 h. Abbreviations: c1—62.5 µg/L; c2—250 µg/L; c3—1000 µg/L; +c—untreated control; −c—negative control (no DNA; and lad − DNA ladder.

Similarly, using the OPB1 primer, Mahaye et al. [27] observed DNA bands characterized by various size ranges compared to the controls following exposure of *P. subcapitata* to citrate- and branched-polyethyleneimine-nAu at 62.5–1000 µg/L for 168 h. The OPB14 primer produced similar RAPD-PCR profiles, irrespective of nAu coating type and exposure duration or concentration. The results of Mahaye et al. [27] indicated that DNA stability decreased after 72 h and increased after 168 h. Thus, they were indicative of likely DNA damage recovery over a long-term exposure period. However, herein, findings for $nCeO_2$ demonstrated persistent DNA damage under extended exposure conditions. This is critical, as genotoxic effects may be, subsequently, transmitted to future generations with deleterious implications such as a compromised defence towards pests or an inability to adopt adverse environmental conditions.

In turn, this may affect survival and reproduction of algae, thus, compromising ecological balance as algae are food source for higher organisms in the food web. For example, transfer of metal oxide ENPs from algae to daphnia [88] or algae to fish [89] have been reported. In addition, the findings imply that high agglomeration of $nCeO_2$ in BG-11 medium does not reduce their reactivity and genotoxicity. These findings indicate that DNA damage on algae is ENPs type dependent. Previous findings have demonstrated irreparable DNA damage where affected cells can trigger cell death by activation of apoptosis to eliminate potentially damaged cells [90]. Conversely, herein, findings from apical endpoints after 168 h (Figures 2 and 3) plausibly indicate cell recovery under chronic conditions compared to 72 h. Metagenomic analysis results have demonstrated that microbial communities can protect themselves and recover their functions through keystone taxa, development of resistance, and resilience and functional redundancy [91]. The findings emphasize the importance of including genotoxicity methods in the risk assessment of ENPs on algae. Furthermore, current findings contribute to the limited body of knowledge on the effects of $nCeO_2$ on algae at low exposure concentrations (µg/L) and long-term exposure conditions, especially using the multi-maker approach that coupled genotoxicity biomarkers with apical endpoints to aid gain complete picture on the effect of these emerging contaminants.

4. Conclusions

$nCeO_2$ at 62.5–1000 µg/L exposure concentrations induced significant algal growth inhibition after 72 h, but growth promotion post 96–168 h, irrespective of exposure concentration. After 72 h, $nCeO_2$ enhanced Chl *a* content compared to the controls at all tested concentrations. However, after 168 h, no significant changes in Chl *a* content were observed between non-exposed and $nCeO_2$–exposed samples ($p > 0.05$). The findings demonstrated that the high agglomeration of smaller-sized $nCeO_2$ do not reduce their reactivity nor hinder their toxicological effects. Furthermore, growth results demonstrated that algal cells could recover under long-term exposure conditions (post 96 h). Assessment of DNA damage using RAPD-PCR showed DNA bands modifications in the form of appearance of new bands and/or disappearance of normal bands compared to the controls. The observed modifications of RAPD-PCR profiles point to likely DNA adducts, DNA breakage, and mutation (point mutations and large rearrangements). In contrast to cell recovery observed after 96 h, DNA damage persisted over 168 h.

Overall, the study provided evidence that exposure duration plays a vital role on the cytotoxic and genotoxic response of *P. subcapitata* to $nCeO_2$. To fully understand the mechanism of ENPs toxicity in algae, we recommend further studies at different endpoints at the molecular (e.g., chromosomal abnormalities, nucleus damage, DNA strand breaks, gene expression) and biochemical (e.g., catalase (CAT), glutathione *S*-transferase (GST), superoxide dismutase (SOD), etc.) levels. Furthermore, studies should be carried out at low environmentally relevant ENPs concentrations using a more realistic exposure medium (e.g., river water) and under chronic exposure conditions to fully understand the long-term impact of $nCeO_2$ on non-target aquatic organisms.

Supplementary Materials: The following supporting information can be downloaded at: https://www.mdpi.com/article/10.3390/toxics11030283/s1, Table S1: The composition of 10% BG-11 medium; Figure S1: Size characterization of nCeO2 (a) TEM images [36], (b) size distribution; Figure S2: Algal growth of *P. subcapitata* at different concentrations of $K_2Cr_2O_7$: Figure S3: in situ $nCeO_2$ concentration (particles/mL) characterization examined using Nanoparticle Tracking Analysis [92].

Author Contributions: Conceptualization: N.M. (Ndeke Musee); methodology, N.M. (Ntombikayise Mahaye); software, N.M. (Ntombikayise Mahaye); validation, N.M. (Ntombikayise Mahaye). and N.M. (Ndeke Musee); formal analysis, N.M. (Ntombikayise Mahaye) and N.M. (Ndeke Musee); investigation, N.M. (Ntombikayise Mahaye); resources, N.M. (Ndeke Musee); data curation, N.M. (Ntombikayise Mahaye); writing—original draft preparation, N.M. (Ntombikayise Mahaye); writing—review and editing, N.M. (Ntombikayise Mahaye) and N.M. (Ndeke Musee); visualization, N.M. (Ntombikayise Mahaye); supervision, N.M. (Ndeke Musee); project administration, N.M. (Ndeke Musee); funding acquisition, N.M. (Ndeke Musee). All authors have read and agreed to the published version of the manuscript.

Funding: This research was funded by the South African National Research Foundation—Department of Science and Technology Professional Development Programme Doctoral Grant (NRF PDP Fellowship UID 88608) (N Mahaye, N Musee), the Council for Scientific and Industrial Research (CSIR), South Africa (ECSD001) (N Mahaye), and the Water Research Commission (WRC) (K5/2509/1) (N Musee, N Mahaye).

Institutional Review Board Statement: Not applicable.

Informed Consent Statement: Not applicable.

Data Availability Statement: Not available.

Conflicts of Interest: The authors declare no conflict of interest.

References

1. Singh, K.R.; Nayak, V.; Sarkar, T.; Singh, R.P. Cerium oxide nanoparticles: Properties, biosynthesis and biomedical application. *RSC Adv.* **2020**, *10*, 27194–27214. [CrossRef] [PubMed]
2. Wu, W.; Li, S.; Liao, S.; Xiang, F.; Wu, X. Preparation of new sunscreen materials Ce1- x Zn x O2- x via solid-state re-action at room temperature and study on their properties. *Rare Metals* **2010**, *29*, 149–153. [CrossRef]
3. Cassee, F.R.; Campbell, A.; Boere, A.J.F.; McLean, S.G.; Duffin, R.; Krystek, P.; Gosens, I.; Miller, M.R. The biological effects of subacute inhalation of diesel exhaust following addition of cerium oxide nanoparticles in atherosclerosis-prone mice. *Environ. Res.* **2012**, *115*, 1–10. [CrossRef]
4. Trovarelli, A. Catalytic Properties of Ceria and CeO_2-Containing Materials. *Catal. Rev.* **1996**, *38*, 439–520. [CrossRef]
5. Wang, C.-H.; Lin, S.-S. Preparing an active cerium oxide catalyst for the catalytic incineration of aromatic hydrocar-bons. *Appl. Catal. A Gen.* **2004**, *268*, 227–233. [CrossRef]
6. Xu, C.; Qu, X. Cerium oxide nanoparticle: A remarkably versatile rare earth nanomaterial for biological applications. *NPG Asia Mater.* **2014**, *6*, e90. [CrossRef]
7. Caputo, F.; De Nicola, M.; Ghibelli, L. Pharmacological potential of bioactive engineered nanomaterials. *Biochem. Pharmacol.* **2014**, *92*, 112–130. [CrossRef] [PubMed]
8. Piccinno, F.; Gottschalk, F.; Seeger, S.; Nowack, B. Industrial production quantities and uses of ten engineered nano-materials in Europe and the world. *J. Nanoparticle Res.* **2012**, *14*, 1109. [CrossRef]
9. Collin, B.; Auffan, M.; Johnson, A.C.; Kaur, I.; Keller, A.A.; Lazareva, A.; Lead, J.R.; Ma, X.; Merrifield, R.C.; Svendsen, C.; et al. Environmental release, fate and ecotoxicological effects of manufactured ceria nanomaterials. *Environ. Sci. Nano* **2014**, *1*, 533–548. [CrossRef]
10. Keller, A.A.; Lazareva, A. Predicted Releases of Engineered Nanomaterials: From Global to Regional to Local. *Environ. Sci. Technol. Lett.* **2013**, *1*, 65–70. [CrossRef]
11. Johnson, A.C.; Park, B. Predicting contamination by the fuel additive cerium oxide engineered nanoparticles within the United Kingdom and the associated risks. *Environ. Toxicol. Chem.* **2012**, *31*, 2582–2587. [CrossRef]
12. Gottschalk, F.; Sun, T.; Nowack, B. Environmental concentrations of engineered nanomaterials: Review of modeling and analytical studies. *Environ. Pollut.* **2013**, *181*, 287–300. [CrossRef]
13. Peters, R.J.; van Bemmel, G.; Milani, N.B.; Hertog, G.C.D.; Undas, A.; van der Lee, M.; Bouwmeester, H. Detection of nanoparticles in Dutch surface waters. *Sci. Total. Environ.* **2017**, *621*, 210–218. [CrossRef]
14. OECD. List of Manufactured Nanomaterials and List of Endpoints for Phase One of the Sponsorship Programme for the Testing of Manufactured Nanomaterials: Revision. 2010. Available online: https://www.oecd.org/chemicalsafety/nanosafety/testing-programme-manufactured-nanomaterials.htm (accessed on 15 January 2023).
15. Abbas, Q.; Liu, G.; Yousaf, B.; Ali, M.U.; Ullah, H.; Munir, M.A.M.; Ahmed, R.; Rehman, A. Biochar-assisted transformation of engineered-cerium oxide nanoparticles: Effect on wheat growth, photosynthetic traits and cerium accumulation. *Ecotoxicol. Environ. Saf.* **2019**, *187*, 109845. [CrossRef]
16. Pulido-Reyes, G.; Briffa, S.M.; Hurtado-Gallego, J.; Yudina, T.; Leganés, F.; Puntes, V.; Valsami-Jones, E.; Rosal, R.; Fernández-Piñas, F. Internalization and toxicological mechanisms of uncoated and PVP-coated cerium oxide nanoparticles in the freshwater *algaChlamydomonas reinhardtii*. *Environ. Sci. Nano* **2019**, *6*, 1959–1972. [CrossRef]
17. Saison, C.; Perreault, F.; Daigle, J.-C.; Fortin, C.; Claverie, J.; Morin, M.; Popovic, R. Effect of core–shell copper oxide nanoparticles on cell culture morphology and photosynthesis (photosystem II energy distribution) in the green alga, *Chlamydomonas reinhardtii*. *Aquat. Toxicol.* **2010**, *96*, 109–114. [CrossRef] [PubMed]
18. Booth, A.; Størseth, T.; Altin, D.; Fornara, A.; Ahniyaz, A.; Jungnickel, H.; Laux, P.; Luch, A.; Sørensen, L. Freshwater dispersion stability of PAA-stabilised cerium oxide nanoparticles and toxicity towards *Pseudokirchneriella subcapitata*. *Sci. Total. Environ.* **2015**, *505*, 596–605. [CrossRef] [PubMed]
19. Rodea-Palomares, I.; Gonzalo, S.; Santiago-Morales, J.; Leganés, F.; García-Calvo, E.; Rosal, R.; Fernández-Piñas, F. An insight into the mechanisms of nanoceria toxicity in aquatic photosynthetic organisms. *Aquat. Toxicol.* **2012**, *122–123*, 133–143. [CrossRef] [PubMed]
20. Wu, D.; Zhang, J.; Du, W.; Yin, Y.; Guo, H. Toxicity mechanism of cerium oxide nanoparticles on cyanobacteria Microcystis aeruginosa and their ecological risks. *Environ. Sci. Pollut. Res.* **2022**, *29*, 34010–34018. [CrossRef]
21. Xie, C.; Ma, Y.; Zhang, P.; Zhang, J.; Li, X.; Zheng, K.; Li, A.; Wu, W.; Pang, Q.; He, X. Elucidating the origin of the toxicity of nano-CeO2 to Chlorella pyrenoidosa: The role of specific surface area and chemical composition. *Environ. Sci. Nano* **2021**, *8*, 1701–1712. [CrossRef]
22. Mahaye, N.; Thwala, M.; Cowan, D.; Musee, N. Genotoxicity of metal based engineered nanoparticles in aquatic organisms: A review. *Mutat. Res. Mol. Mech. Mutagen.* **2017**, *773*, 134–160. [CrossRef] [PubMed]
23. Milani, Z.M.; Charbgoo, F.; Darroudi, M. Impact of physicochemical properties of cerium oxide nanoparticles on their toxicity effects. *Ceram. Int.* **2017**, *43*, 14572–14581. [CrossRef]
24. Lee, S.-W.; Kim, S.-M.; Choi, J. Genotoxicity and ecotoxicity assays using the freshwater crustacean Daphnia magna and the larva of the aquatic midge Chironomus riparius to screen the ecological risks of nanoparticle exposure. *Environ. Toxicol. Pharmacol.* **2009**, *28*, 86–91. [CrossRef]

25. Bayat, N. Toxicity and Biological Impact of Metal and Metal Oxide Nanoparticles Focus on the Vascular Toxicity of ul-tra-Small Titanium Dioxide Nanoparticles. Department of Biochemistry and Biophysics, Stockholm University: Stockholm, Sweden, 2015.
26. Taylor, N.S.; Merrifield, R.; Williams, T.D.; Chipman, J.K.; Lead, J.R.; Viant, M.R. Molecular toxicity of cerium oxide nanoparticles to the freshwater alga *Chlamydomonas reinhardtii* is associated with supra-environmental exposure concentra-tions. *Nanotoxicology* **2016**, *10*, 32–41.
27. Mahaye, N.; Leareng, S.K.; Musee, N. Cytotoxicity and genotoxicity of coated-gold nanoparticles on freshwater algae *Pseudokirch-neriella subcapitata*. *Aquat. Toxicol.* **2021**, *236*, 105865. [CrossRef] [PubMed]
28. Mahana, A.; Guliy, O.I.; Mehta, S.K. Accumulation and cellular toxicity of engineered metallic nanoparticle in freshwater microalgae: Current status and future challenges. *Ecotoxicol. Environ. Saf.* **2021**, *208*, 111662. [CrossRef]
29. Yingjun, W.; Jia, L.; Yun, L.Ü.; Hangbiao, J.; Shihuai, D.; Yunmin, Z. Effects of cerium on growth and physiological characteristics of *Anabaena flosaquae*. *J. Rare Earths* **2012**, *30*, 1287–1292.
30. Xue, W.; Yousheng, L.; Dongwu, L.; Hengjian, X.; Tao, L.; Fengyun, Z. Cerium toxici-ty, uptake and translocation in *Arabidopsis thaliana* seedlings. *J. Rare Earths* **2012**, *30*, 579–585.
31. Angel, B.M.; Vallotton, P.; Apte, S.C. On the mechanism of nanoparticulate CeO2 toxicity to freshwater algae. *Aquat. Toxicol.* **2015**, *168*, 90–97. [CrossRef] [PubMed]
32. Vannini, C.; Domingo, G.; Marsoni, M.; De Mattia, F.; Labra, M.; Castiglioni, S.; Bracale, M. Effects of a complex mixture of therapeutic drugs on unicellular algae *Pseudokirchneriella subcapitata*. *Aquat. Toxicol.* **2011**, *101*, 459–465. [CrossRef] [PubMed]
33. Rocco, L.; Santonastaso, M.; Nigro, M.; Mottola, F.; Costagliola, D.; Bernardeschi, M.; Guidi, P.; Lucchesi, P.; Scarcelli, V.; Corsi, I.; et al. Genomic and chromosomal damage in the marine mussel Mytilus galloprovincialis: Effects of the combined exposure to titanium dioxide nanoparticles and cadmium chloride. *Mar. Environ. Res.* **2015**, *111*, 144–148. [CrossRef] [PubMed]
34. Rocco, L.; Valentino, I.V.; Scapigliati, G.; Stingo, V. RAPD-PCR analysis for molecular characterization and genotoxic studies of a new marine fish cell line derived from Dicentrarchus labrax. *Cytotechnology* **2013**, *66*, 383–393. [CrossRef]
35. Rocco, L.; Santonastaso, M.; Mottola, F.; Costagliola, D.; Suero, T.; Pacifico, S.; Stingo, V. Genotoxicity assessment of TiO2 nanoparticles in the teleost Danio rerio. *Ecotoxicol. Environ. Saf.* **2015**, *113*, 223–230. [CrossRef]
36. Mahaye, N. Stability of Gold and Cerium Oxide Nanoparticles in Aqueous Environments, and Their Effects on Pseudo-kirchneriella Subcapitata and Salvinia Minima. Ph.D. Thesis, University of Pretoria, Pretoria, South Africa, 2019. Available online: https://repository.up.ac.za/handle/2263/72778 (accessed on 15 January 2023).
37. Slabbert, L. *Methods for Direct Estimation of Ecological Effect Potential (DEEEP)*, 1st ed.; Water Research Com-mission Report No.: 1313/01/04; Water Research Commission: Pretoria, South Africa, 2004; p. 100.
38. Rodrigues, L.H.R.; Arenzon, A.; Raya-Rodriguez, M.T.; Fontoura, N.F. Algal density assessed by spectrophotometry: A calibration curve for the unicellular algae *Pseudokirchneriella subcapitata*. *J. Environ. Chem. Ecotoxicol.* **2011**, *3*, 225–228.
39. Miller, W.E.; Greene, J.C.; Shiroyama, T. *The Selenastrum capricornutum printz algal assay bottle test: Experimental design, application, and data interpretation protocol*; Environmental Protection Agency, Office of Research and Develop-ment, Corvallis Environmenal Research Laboratory: Washington, DC, USA, 1978.
40. Markus, A.; Krystek, P.; Tromp, P.; Parsons, J.; Roex, E.; de Voogt, P.; Laane, R. Determination of metal-based nanoparticles in the river Dommel in the Netherlands via ultrafiltration, HR-ICP-MS and SEM. *Sci. Total. Environ.* **2018**, *631–632*, 485–495. [CrossRef] [PubMed]
41. de Klein, J.J.M.; Quik, J.T.K.; Bäuerlein, P.S.; Koelmans, A.A. Towards validation of the NanoDUFLOW nanoparticle fate model for the river Dommel, The Netherlands. *Environ. Sci. Nano* **2016**, *3*, 434–441. [CrossRef]
42. Giese, B.; Klaessig, F.; Park, B.; Kaegi, R.; Steinfeldt, M.; Wigger, H.; von Gleich, A.; Gottschalk, F. Risks, Release and Concentrations of Engineered Nanomaterial in the Environment. *Sci. Rep.* **2018**, *8*, 1–18. [CrossRef]
43. Grillo, R.; Clemente, Z.; de Oliveira, J.L.; Campos, E.V.R.; Chalupe, V.C.; Jonsson, C.M.; de Lima, R.; Sanches, G.; Nishisaka, C.S.; Rosa, A.H.; et al. Chitosan nanoparticles loaded the herbicide paraquat: The influence of the aquatic humic substances on the colloidal stability and toxicity. *J. Hazard. Mater.* **2015**, *286*, 562–572. [CrossRef] [PubMed]
44. Ozkaleli, M.; Erdem, A. Biotoxicity of TiO2 Nanoparticles on Raphidocelis subcapitata Microalgae Exemplified by Membrane Deformation. *Int. J. Environ. Res. Public Heal.* **2018**, *15*, 416. [CrossRef]
45. Harris, E.H. *The Chlamydomonas Sourcebook*; Academic Press: San Diego, CA, USA, 1989. [CrossRef]
46. A Atienzar, F.; Venier, P.; Jha, A.; Depledge, M.H. Evaluation of the random amplified polymorphic DNA (RAPD) assay for the detection of DNA damage and mutations. *Mutat. Res. Toxicol. Environ. Mutagen.* **2002**, *521*, 151–163. [CrossRef]
47. Nur, Y.; Lead, J.; Baalousha, M. Evaluation of charge and agglomeration behavior of TiO2 nanoparticles in ecotoxicological media. *Sci. Total. Environ.* **2015**, *535*, 45–53. [CrossRef] [PubMed]
48. Alam, B.; Philippe, A.; Rosenfeldt, R.R.; Seitz, F.; Dey, S.; Bundschuh, M.; Schaumann, G.E.; Brenner, S.A. Synthesis, characteriza-tion, and ecotoxicity of CeO2 nanoparticles with differing properties. *J. Nanoparticle Res.* **2016**, *18*, 1–10. [CrossRef]
49. Oriekhova, O.; Stoll, S. Stability of uncoated and fulvic acids coated manufactured CeO2 nanoparticles in various conditions: From ultrapure to natural Lake Geneva waters. *Sci. Total. Environ.* **2016**, *562*, 327–334. [CrossRef]
50. Yang, X.; Pan, H.; Wang, P.; Zhao, F.-J. Particle-specific toxicity and bioavailability of cerium oxide (CeO2) nanoparticles to *Arabidopsis thaliana*. *J. Hazard. Mater.* **2017**, *322*, 292–300. [CrossRef] [PubMed]
51. Song, U.; Shin, M.; Lee, G.; Roh, J.; Kim, Y.; Lee, E.J. Functional Analysis of TiO2 Nanoparticle Toxicity in Three Plant Species. *Biol. Trace Element Res.* **2013**, *155*, 93–103. [CrossRef] [PubMed]

52. Zhang, P.; Ma, Y.; Liu, S.; Wang, G.; Zhang, J.; He, X.; Zhang, J.; Rui, Y.; Zhang, Z. Phytotoxicity, uptake and transformation of nano-CeO2 in sand cultured romaine lettuce. *Environ. Pollut.* **2017**, *220*, 1400–1408. [CrossRef]
53. Rogers, N.J.; Franklin, N.M.; Apte, S.C.; Batley, G.E.; Angel, B.; Lead, J.R.; Baalousha, M. Physico-chemical behaviour and algal toxicity of nanoparticulate CeO2 in freshwater. *Environ. Chem.* **2010**, *7*, 50–60. [CrossRef]
54. Manier, N.; Bado-Nilles, A.; Delalain, P.; Aguerre-Chariol, O.; Pandard, P. Ecotoxicity of non-aged and aged CeO2 nanomaterials towards freshwater microalgae. *Environ. Pollut.* **2013**, *180*, 63–70. [CrossRef]
55. Yu, Q.; Wang, Z.; Zhai, Y.; Zhang, F.; Vijver, M.G.; Peijnenburg, W.J. Effects of humic substances on the aqueous sta-bility of cerium dioxide nanoparticles and their toxicity to aquatic organisms. *Sci. Total Environ.* **2021**, *781*, 146583. [CrossRef]
56. Hitchman, A.; Smith, G.H.S.; Ju-Nam, Y.; Sterling, M.; Lead, J.R. The effect of environmentally relevant conditions on PVP stabilised gold nanoparticles. *Chemosphere* **2013**, *90*, 410–416. [CrossRef]
57. Lowry, G.V.; Hill, R.J.; Harper, S.; Rawle, A.F.; Hendren, C.O.; Klaessig, F.; Nobbmann, U.; Sayre, P.; Rumble, J. Guidance to improve the scientific value of zeta-potential measurements in nanoEHS. *Environ. Sci. Nano* **2016**, *3*, 953–965. [CrossRef]
58. Rioboo, C.; Prado, R.; Herrero, C.; Cid, A. Population growth study of the rotifer Brachionus sp. fed with triazine-exposed microalgae. *Aquat. Toxicol.* **2007**, *83*, 247–253. [CrossRef]
59. Dubey, D.; Dutta, V. Nutrient Enrichment in Lake Ecosystem and Its Effects on Algae and Macrophytes. *Environ. Concerns Sustain. Dev. Vol. 2 Biodivers. Soil Waste Manag.* **2019**, 81–126. [CrossRef]
60. Dedman, C.J.; Rizk, M.M.I.; Christie-Oleza, J.A.; Davies, G.-L. Investigating the Impact of Cerium Oxide Nanoparticles Upon the Ecologically Significant Marine Cyanobacterium Prochlorococcus. *Front. Mar. Sci.* **2021**, *8*, 668097. [CrossRef]
61. Röhder, L.A.; Brandt, T.; Sigg, L.; Behra, R. Influence of agglomeration of cerium oxide nanoparticles and speciation of cerium(III) on short term effects to the green algae Chlamydomonas reinhardtii. *Aquat. Toxicol.* **2014**, *152*, 121–130. [CrossRef]
62. Zemke-White, W.L.; Clements, K.D.; Harris, P.J. Acid lysis of macroalgae by marine herbivorous fishes: Effects of acid pH on cell wall porosity. *J. Exp. Mar. Biol. Ecol.* **2000**, *245*, 57–68. [CrossRef]
63. Deng, X.-Y.; Cheng, J.; Hu, X.-L.; Wang, L.; Li, D.; Gao, K. Biological effects of TiO2 and CeO2 nanoparticles on the growth, photosynthetic activity, and cellular components of a marine diatom Phaeodactylum tricornutum. *Sci. Total. Environ.* **2017**, *575*, 87–96. [CrossRef] [PubMed]
64. Zhao, G.; Wu, D.; Cao, S.; Du, W.; Yin, Y.; Guo, H. Effects of CeO2 Nanoparticles on Microcystis aeruginosa Growth and Microcystin Production. *Bull. Environ. Contam. Toxicol.* **2020**, *104*, 834–839. [CrossRef]
65. Du, S.; Zhang, P.; Zhang, R.; Lu, Q.; Liu, L.; Bao, X.; Liu, H. Reduced graphene oxide induces cytotoxicity and inhibits photosynthetic performance of the green alga Scenedesmus obliquus. *Chemosphere* **2016**, *164*, 499–507. [CrossRef]
66. Qian, H.; Zhu, K.; Lu, H.; Lavoie, M.; Chen, S.; Zhou, Z.; Deng, Z.; Chen, J.; Fu, Z. Contrasting silver nanoparticle toxicity and detoxification strategies in Microcystis aeruginosa and Chlorella vulgaris: New insights from proteomic and physiological analyses. *Sci. Total. Environ.* **2016**, *572*, 1213–1221. [CrossRef]
67. Chiu, M.-H.; Khan, Z.A.; Garcia, S.G.; Le, A.D.; Kagiri, A.; Ramos, J.; Tsai, S.-M.; Drobenaire, H.W.; Santschi, P.; Quigg, A.; et al. Effect of Engineered Nanoparticles on Exopolymeric Substances Release from Marine Phytoplankton. *Nanoscale Res. Lett.* **2017**, *12*, 620. [CrossRef]
68. Wang, S.; Lv, J.; Ma, J.; Zhang, S. Cellular internalization and intracellular biotransformation of silver nanoparticles in *Chlamydomonas reinhardtii*. *Nanotoxicology* **2016**, *10*, 1129–1135. [CrossRef] [PubMed]
69. Metzler, D.M.; Erdem, A.; Tseng, Y.H.; Huang, C.P. Responses of Algal Cells to Engineered Nanoparticles Measured as Algal Cell Population, Chlorophyll a, and Lipid Peroxidation: Effect of Particle Size and Type. *J. Nanotechnol.* **2012**, *2012*, 237284. [CrossRef]
70. Li, F.; Liang, Z.; Zheng, X.; Zhao, W.; Wu, M.; Wang, Z. Toxicity of nano-TiO2 on algae and the site of reactive oxygen species production. *Aquat. Toxicol.* **2015**, *158*, 1–13. [CrossRef]
71. Franqueira, D.; Orosa, M.; Torres, E.; Herrero, C.; Cid, A. Potential use of flow cytometry in toxicity studies with microalgae. *Sci. Total. Environ.* **2000**, *247*, 119–126. [CrossRef]
72. Eullaffroy, P.; Vernet, G. The F684/F735 chlorophyll fluorescence ratio: A potential tool for rapid detection and determination of herbicide phytotoxicity in algae. *Water Res.* **2003**, *37*, 1983–1990. [CrossRef]
73. Hazeem, L.J.; Bououdina, M.; Rashdan, S.; Brunet, L.; Slomianny, C.; Boukherroub, R. Cumulative effect of zinc oxide and titanium oxide nanoparticles on growth and chlorophyll a content of Picochlorum sp. *Environ. Sci. Pollut. Res.* **2015**, *23*, 2821–2830. [CrossRef] [PubMed]
74. Hong, F.; Zhou, J.; Liu, C.; Yang, F.; Wu, C.; Zheng, L.; Yang, P. Effect of Nano-TiO2 on Photochemical Reaction of Chloroplasts of Spinach. *Biol. Trace Element Res.* **2005**, *105*, 269–280. [CrossRef]
75. Lei, Z.; Mingyu, S.; Xiao, W.; Chao, L.; Chunxiang, Q.; Liang, C.; Hao, H.; Xiaoqing, L.; Fashui, H. Effects of Nano-anatase on Spectral Characteristics and Distribution of LHCII on the Thylakoid Membranes of Spinach. *Biol. Trace Element Res.* **2007**, *120*, 273–283. [CrossRef]
76. Hartmann, N.B. Algal testing of titanium dioxide nanoparticles—Testing considerations, inhibitory effects and modification of cadmium bioavailability 8. *Toxicology* **2010**, *269*, 190–197. [CrossRef] [PubMed]
77. Chen, L.; Zhou, L.; Liu, Y.; Deng, S.; Wu, H.; Wang, G. Toxicological effects of nanometer titanium dioxide (nano-TiO2) on *Chlamydomonas reinhardtii*. *Ecotoxicol. Environ. Saf.* **2012**, *84*, 155–162. [CrossRef]
78. Gui, X.; Rui, M.; Song, Y.; Ma, Y.; Rui, Y.; Zhang, P.; He, X.; Li, Y.; Zhang, Z.; Liu, L. Phytotoxicity of CeO2 nanoparticles on radish plant (Raphanus sativus). *Environ. Sci. Pollut. Res.* **2017**, *24*, 13775–13781. [CrossRef]

79. Wang, Y.; Wang, L.; Ma, C.; Wang, K.; Hao, Y.; Chen, Q.; Mo, Y.; Rui, Y. Effects of cerium oxide on rice seed-lings as affected by co-exposure of cadmium and salt. *Environ. Pollut.* **2019**, *252*, 1087–1096. [CrossRef]
80. Navarro, E.; Piccapietra, F.; Wagner, B.; Marconi, F.; Kaegi, R.; Odzak, N.; Sigg, L.; Behra, R. Toxicity of Silver Nanoparticles to *Chlamydomonas reinhardtii*. *Environ. Sci. Technol.* **2008**, *42*, 8959–8964. [CrossRef]
81. Schwabe, F.; Schulin, R.; Limbach, L.K.; Stark, W.; Bürge, D.; Nowack, B. Influence of two types of organic matter on interaction of CeO2 nanoparticles with plants in hydroponic culture. *Chemosphere* **2013**, *91*, 512–520. [CrossRef] [PubMed]
82. Lukhele, L.P.; Mamba, B.; Musee, N.; Wepener, V. Acute Toxicity of Double-Walled Carbon Nanotubes to Three Aquatic Organisms. *J. Nanomater.* **2015**, *2015*, 219074. [CrossRef]
83. Quigg, A.; Chin, W.C.; Chen, C.S.; Zhang, S.; Jiang, Y.; Miao, A.J.; Schwehr, K.A.; Xu, C.; Santschi, P.H. Direct and indirect toxic effects of engineered nanoparticles on algae: Role of natural organic matter. *ACS Sustain. Chem. Eng.* **2013**, *1*, 686–702. [CrossRef]
84. Von Moos, N.; Slaveykova, V.I. Oxidative stress induced by inorganic nanoparticles in bacteria and aquatic microalgae—State of the art and knowledge gaps. *Nanotoxicology* **2013**, *8*, 605–630. [CrossRef]
85. Chen, F.; Xiao, Z.; Yue, L.; Wang, J.; Feng, Y.; Zhu, X.; Wang, Z.; Xing, B. Algae response to engineered nano-particles: Current understanding, mechanisms and implications. *Environ. Sci. Nano* **2019**, *6*, 1026–1042. [CrossRef]
86. Atienzar, F.A.; Jha, A.N. The random amplified polymorphic DNA (RAPD) assay and related techniques applied to genotoxicity and carcinogenesis studies: A critical review. *Mutat. Res. Mol. Mech. Mutagen.* **2006**, *613*, 76–102. [CrossRef]
87. Załęska-Radziwiłł, M.; Doskocz, N. DNA changes in *Pseudomonas putida* induced by aluminum oxide nanoparticles using RAPD analysis. *Desalination Water Treat.* **2015**, *57*, 1573–1581. [CrossRef]
88. Chen, X.; Zhu, Y.; Yang, K.; Zhu, L.; Lin, D. Nanoparticle TiO2 size and rutile content impact bioconcentration and biomagnification from algae to daphnia. *Environ. Pollut.* **2019**, *247*, 421–430. [CrossRef] [PubMed]
89. Xin, X.; Huang, G.; Zhang, B.; Zhou, Y. Trophic transfer potential of nTiO2, nZnO, and triclosan in an algae-algae eating fish food chain. *Aquat. Toxicol.* **2021**, *235*, 105824. [CrossRef] [PubMed]
90. Matt, S.; Hofmann, T.G. The DNA damage-induced cell death response: A roadmap to kill cancer cells. *Cell. Mol. Life Sci.* **2016**, *73*, 2829–2850. [CrossRef] [PubMed]
91. Xiong, J.-Q.; Cui, P.; Ru, S.; Kurade, M.B.; Patil, S.M.; Yadav, K.K.; Fallatah, A.M.; Cabral-Pinto, M.M.; Jeon, B.-H. A comprehensive review on the effects of engineered nanoparticles on microalgal treatment of pollutants from wastewater. *J. Clean. Prod.* **2022**, *344*, 131121. [CrossRef]
92. Nyati, S.; Werth, S.; Honegger, R. Genetic Diversity of Sterile Cultured Trebouxia Photobionts Associated with the Lichen-Forming Fungus Xanthoria Parietina Visualized with RAPD-PCR Fingerprinting Techniques. *The Lichenologist* **2013**, *344*, 825–840. [CrossRef]